MVA '96 IAPR Workshop on Machine Vision Applications, November. 12-14, 1996, Tokyo, Japan

Energy-based Method for Road Extraction from Satellite Images

Ke Qifa* Xiao Jing Yang Zhiyong

Songde MA†

National Laboratory of Pattern Recognition

Institute of Automation, Chinese Academy of Sciences

Abstract

In this paper, we present a new method for automatic road tracking and extraction from satellite images. Our method is a kind of global and parallel method. It includes the following three parts: 1) an edge detector is applied and the satellite image is transfered into binary edge map (EM). 2) we propose a special kind of energy function with marginal effect to represent each edge chain in the EM. Through this energy function, we are able to track and extract the candidates of roads. 3) By applying the generic knowledge of roads, we can easily discard the false candidates, and then produce the road boundaries from the remaining chains. The experiments show that our method can extract the roads from the satellite images robustly and quickly. It is also shown that our method can be extended to extract the linear features in other kinds of images.

1 Introduction

During the past, much effort has been concerntrated on automatic road extraction from satellite or aerial images, in which a tracking algorithm was used to connect all the edge points along the road. In the presence of noise, tracking is the main difficult problem in road extraction because edge points along the road are not necessarily connected in the original edge map. In each step of tracking, we must make the decision of "What is the next point of the road?". Most of the existing methods, such as generic edge detectors[1, 2], crest detectors, morphological operators[3] and "Duda-Road-Operator"[4], are local methods since only the local information of the current terminal point is used to make the decision. In the presence of noise, these tracking strategies would result in wrong decision. Kalman filter or other linear prediction methods can be used to reduce the wrong decision, but since a road is not always locally linear, the linear prediction methods are not always successful. In [5], a tracking method is presented which uses more global imformation. Donald Geman etc[6] proposed a model-based method for road tracking. Given the starting point and direction, this method can track the main road based on a statistical model.

To our human eyes, roads can be easily extracted since we can find the global saliency of roads. In this paper, we propose an energy function to represent this saliency. Based on the energy function, we present a new and efficient method for road tracking and extraction. Our method consists of the following three parts: 1) An edge detector is applied to transfer the original satellite image to binary edge map (EM). We can see from the EM that all the roads are immerged in the background and the roads are, in general, broken into many segments. 2) We utilize our energy function to track the road chains and integrate the broken road segments into a set of new edge chains. We then compute the saliency of each new chain via the energy function and rank the chains according to their saliency. The most salient chains are considered as the candidates of roads. 3) Through the generic knowledge about the road, we can easily discard the false road chains, and then producing the road boundaries from the remaining chains. We can see that our method is very efficient without heuristic search.

2 Energy functional for road tracking and extraction

Human eyes can easily extract roads in the satellite images, while such task is very difficult for computers. We argue that it is because human eyes can easily catch the global saliency of roads to extract them. In this section, we propose an energy function to represent this saliency which is the basis of our method.

2.1 Energy functional

We propose the following functional to represent the energy of a solitary line contour $l(s) = (x(s), y(s))$[9],where (x, y) is the Euclidean cooradinate:

$$\begin{aligned} H(l) &= 2h_0 + \tfrac{1}{2}\int_\Omega k(s)(\nabla l(s))^2 ds \\ &+ \tfrac{1}{2}\int_\Omega b(s)(\nabla^2 l(s))^2 ds \end{aligned} \tag{1}$$

*Address: P. O. Box 2728, Beijing 100080, P.R. China E-mail: keq@prlsun7.ia.ac.cn

†E-mail: masd@prlsun2.ia.ac.cn

where s is the arc length parameter ranging on $\Omega = [0, L]$, L is the length of the line contour. $k(s)$ and $b(s)$ are elastic coefficients. We denote $\nabla l(s) = \left(\frac{\partial x}{\partial s}, \frac{\partial y}{\partial s}\right)$ and $\nabla^2 l(s) = \left(\frac{\partial^2 x}{\partial s^2}, \frac{\partial^2 y}{\partial s^2}\right)$. The first term is the energy for two end points of $l(s)$, the second and the third term are due to stretching modes and bending modes respectively. Note that in [10, 11] $k(s)$ and $b(s)$ are constant coefficients while they are the functions of arc length parameter s here. More details concerning Eq.(1) are referred to [9]. Since in this paper s is arc length parameter, we have $(\nabla l(s))^2 = \nabla l(s) \cdot \nabla l(s) = 1$[12]. So, Eq.(1) can be rewritten as:

$$H(l) = 2h_0 + \frac{1}{2}\int_{\Omega} k(s)ds + \frac{1}{2}\int_{\Omega} b(s)(\nabla^2 l(s))^2 ds \tag{2}$$

A line contour can be segmented into a set of segments consisting of two sets: straight lines as set 1 and arcs as set 2[13, 14, 15]. Since $\nabla^2 l(s) = 0$ in set 1 and $\left(\nabla^2 l(s)\right)^2 = \nabla^2 l(s) \cdot \nabla^2 l(s) = \frac{1}{r_i^2} = c_i$ in set 2[12], where r_i is the radius of the i^{th} arc segment in set 2, the energy functional can be represented as:

$$\begin{array}{l} H(l) = \sum h_0 + \sum_{i \in 1} \int_{\Omega_i} K(s)ds \\ + \sum_{i \in 2} \int_{\Omega_i} K(s)ds + \sum_{i \in 2} \int_{\Omega_i} c_i B(s)ds \end{array} \tag{3}$$

where $K(s) = \frac{1}{2}k(s)$ and $B(s) = \frac{1}{2}b(s)$. The subscripts of summations refer to sum all the segments of set 1 and 2 respectively, and Ω_i is the parameter interval of the i^{th} segment. Note that $K(s)$ and $B(s)$ are independent on $l(s)$. The representation of a given contour using Eq.(3) is different from using Eq.(1) and we argue that Eq.(3) is more reasonalble[13, 14, 15]. In addition, since $K(s)$ and $B(s)$ are independent on the given contour $l(s)$, the computation of the energy of different contours can be fulfilled in an easy and fast way.

2.2 Energy representation with marginal effect property

Consider a special case. Suppose that the given contour $l(s)$ is a straight line with length of L. According to Eq.(3), the energy representation of $l(s)$ is:

$$H(l) = 2h_0 + \int_0^L K(s)ds \tag{4}$$

Consider *the increase of* $H(l)$(denoted by dH) when the length of $l(s)$ has an increase of $\triangle s$. From Eq.(4), we have:

$$dH \approx \left.\frac{\partial H}{\partial s}\triangle s\right|_{s=L} = K(s)\triangle s|_{s=L} \tag{5}$$

If $l(s)$ is an arc segment with length L, we have:

$$dH \approx \left.\frac{\partial H}{\partial s}\triangle s\right|_{s=L} = B(s)\triangle s|_{s=L} \tag{6}$$

If $K(s)$ and $B(s)$ in Eq.(3) are monotonously decreasing functions, that is:

$$K(s_1)\triangle s < K(s_2)\triangle s, B(s_1)\triangle s < B(s_2)\triangle s \tag{7}$$

then we have $dH\,|_{s=s_1} < dH|_{s=s_2}$, where $s_1 > s_2$. This means that with the increasing of the total length of $l(s)$, the energy increase resulted from the unit length increase at the end of $l(s)$ is decreasing, such characteristic of energy increase is called marginal effect property. So we call the increase $K(s)\triangle s, B(s)\triangle s$ marginal energy, and the energy representation of Eq.(3) has marginal effect property. This term is borrowed from economical analysis where it is called marginal utility which is one of the foundations of modern mathematical economics[8].

Note that only after we have done the decomposition of Eq.(3) can the marginal effect be explicitly expressed and be meaningful. So, marginal effect is related to geometric redundancy reduction.

We now consider a special case. We choose:

$$K(s) = c_1' s^{\beta}, \quad B(s) = c_2' s^{\beta} \tag{8}$$

where $-1 < \beta < 0$ and c_1', c_2' are constant coeffcients,$c_1' < c_2'$. Then Eq.(3) can be rewritten as:

$$H(l) = \sum h_0 + c_1 \sum_{i \in 1,2} a_i^{\alpha} + c_2 \sum_{i \in 2} c_i a_i^{\alpha} \tag{9}$$

where $0 < \alpha = 1 + \beta < 1$, a_i is the length of the i^{th} segment and $c_1 = \frac{c_1'}{1+\beta}, c_2 = \frac{c_2'}{1+\beta}, c_i = \frac{1}{r_i^2}, r_i$ is the radius of the i^{th} arc segment in set 2. It is obvious that $K(s)$ and $B(s)$ we choose here satisfies Eq.(7), so the energy representation of (9) has marginal effect property. The exponent α represents the amplitude of marginal effect. The greater $(1 - \alpha)$, the greater the marginal effect.

2.3 Modified energy function and unit length energy

In real image, after edge detection, edge tracing and edge chain decomposition, a road boundary is decomposed into n line or arc segments, which are called road segments in the following sections. These n road segments in the edge map are not always aligned on a straight line, so we should consider the turning angles between two segments. In addition, some road segments are arc segments, which should be also considered now.

2.3.1 Consider the turning angle

Consider a segment l (straigh line or arc) of length a. Suppose that the increase of $\triangle s$ at the end of l forms an angle of θ with the tangent at the end of l. According to Eq.(9), the energy of l with length a is: $H(a) = 2h_0 + ca^{\alpha}$, where $c = c_1 + \frac{1}{r^2}c_2$ if l is an arc segment with radius of r, otherwise $c = c_1$. Such discrimination makes no difference in the following formula. When $\theta = 0$, the energy of $a + \triangle s$ is: $H(a+\triangle s) = 2h_0 + (a+\triangle s)^\alpha$. The marginal effect property means:

$$\frac{2h_0 + c(a+\triangle s)^\alpha}{a+\triangle s} < \frac{2h_0 + ca^\alpha}{a} \tag{10}$$

The inequality of (10) is satisfied if $0 < \alpha < 1$.

When $\theta \neq 0$, we only consider the case of $|\theta| < \frac{\pi}{2}$, which is reasonable since in the images the road is modeled as a discretization of a smooth, planar curve whose curvature is bounded by a known value [6]. We assume the following formula to represent the energy of $l(a+\triangle s)$:

$$H(a+\triangle s) = 2h_0 + c\left(a + \frac{\triangle s}{\cos\theta}\right)^\alpha \tag{11}$$

Again, to have the marginal effect property, the energy representation of Eq.(11) should satisfy:

$$\frac{2h_0 + c\left(a + \frac{\triangle s}{\cos\theta}\right)^\alpha}{a+\triangle s} < \frac{2h_0 + ca^\alpha}{a}.$$

We get:

$$|\theta| < \cos^{-1}\alpha, \quad 0 < \alpha < 1 \tag{12}$$

2.3.2 consider the basic case of two segments with a small gap in between

Our algorithm is an update process (see section 3.2 for details). In each step, we only need to consider two segments with a gap in between. The two segments are denoted as l_1 and l_2 with length of a_1 and a_2 respectively. b is the gap length between l_1 and l_2. θ_1 is the turning angle between l_1 and b, θ_2 the turning angle between b an l_2. There exists the following three cases:

(i) l_1 and l_2 are all straight line segments.

The total energy of l_1 and l_2 is:

$$H_1 = H(l_1) + H(l_2) = 4h_0 + c_1 a_1^\alpha + c_1 a_2^\alpha$$

If $|\theta_1| < \theta_T, |\theta_2| < \theta_T$, θ_T is a predefined angle which satisfies Eq.(12), we fill the gap to connect them and produce a new line. We propose the following formula to represent the energy representation of the new line according to Eq.(11):

$$H_2 = 4h_0 + c_1\left(a_1 + a_2 + \frac{k_1 b}{\cos\theta_1} + \frac{k_2 b}{\cos\theta_2}\right)^\alpha + \bar{c}b^\alpha \tag{13}$$

where $k_1 = k_2 = 1/2$ if $\theta_1 = \theta_2 = 0$, otherwise $k_1 = \frac{\theta_2}{\theta_1+\theta_2}, k_2 = \frac{\theta_1}{\theta_1+\theta_2}$. If $H_2 < H_1$, we accept the above grouping and denote it as *true connection.* If $H_2 > H_1$, we couldn't group l_1 and l_2 as a straight line. However, we remember such grouping and denote it as *false connection.* According to Eq.(11), the energy of it is:

$$\begin{aligned} H_2 &= 4h_0 + c_1\left(a_1 + \tfrac{b_1}{\cos\theta_1}\right)^\alpha \\ &+ c_1\left(a_2 + \tfrac{b_2}{\cos\theta_2}\right)^\alpha + \bar{c}b^\alpha \end{aligned} \tag{14}$$

where $b_1 = \frac{\theta_2}{\theta_1+\theta_2}b, b_2 = \frac{\theta_1}{\theta_1+\theta_2}b$. It is obvious that $H_2 > H_1$. If $|\theta_1| > \theta_T$ or $|\theta_2| > \theta_T$, connection of l_1 and l_2 is refused.

(ii) l_1 and l_2 are all arc segments. According to Eq.(9), the total energy of l_1 and l_2 is:

$$\begin{aligned} H_1 &= H(l_1) + H(l_2) \\ &= 4h_0 + \left(c_1 + \tfrac{c_2}{r_1^2}\right)a_1^\alpha + \left(c_1 + \tfrac{c_2}{r_1^2}\right)a_2^\alpha \end{aligned} \tag{15}$$

where r_1 and r_2 are radius of l_1 and l_2 respectively. If $|\theta_1| < \theta_T, |\theta_2| < \theta_T$ and $|r_1 - r_2| < \varepsilon$, where ε is a small real, we fill the gap and group them as a single arc. The energy representation H_2 of new arc is same as Eq.(13) except that c_1 is replaced by $\left(c_1 + \frac{c_2}{(\frac{r_1+r_2}{2})^2}\right)$.

If $H_2 < H_1$, such grouping is accepted and denoted as true connection. If $H_2 > H_1$, we denote such connection as false connection. If $|\theta_1| > \theta_T$ or $|\theta_2| > \theta_T$ or $|r_1 - r_2| > \varepsilon$, connection of l_1 and l_2 is refused.

(iii) l_1 is an arc (straight line) and l_2 is a straight line (arc). If the radius of l_1 is very large, we approximate it using a straight line with the same length and this is the case of (i). Otherwise we refuse the connection of l_1 and l_2.

2.3.3 Global saliency

Our algorithm is an update processing. In each step we consider two segments. If the grouping of these two segments is accepted and a new segment is formed, which is the input of the following iteration (see section 3.2 for detail)

After the connection process (grouping), we define the global saliency of each group as the *energy of unit length (EUL).*

$$EUL = \frac{H}{L}, \quad L = \sum_{i=1}^{n} a_i + \sum_{i=1}^{n-1} b_i \tag{16}$$

The smaller EUL, the more salient of this group. We rank the groups according to their saliency and then choose the most salient groups as the feature we want to extract.

3 Experiment results

The brief description of our algorithm is given in the section of introduction, details are given in [7] and are omitted here for the lack of space. We have applied our method to several images, the experiment results are satisfactory.

Fig.1a is an satellite image with some roads immerged in a complicated background. Fig.1b is the final result. It takes about 3 seconds in Sparc10 station to produce Fig.1b. The result is insensitive to resonable changes of the parameters in Eq.(14). We find that almost all of the roads are successfully tracked and extracted. Fig.2a is an aerial image but with curve-like roads in it. Fig.2b is the final result using our method. As can be seen from Fig.1 and 2, our method can successfully extract the straighted or curve-like roads from satellite or aerial images.

4 Extension of our method and conclusion

In fact, our method can be extended to extract linear-features in other kinds of images, such as the blood vessel extraction from medical images.

Fig.3a is a medical image (2D medical angiogram), Fig.3b is the final result using our method. As can be seen, the network of vessels is exactly detected.

By utilizing the marginal property of the energy representation, we are able to use the global saliency to track and extract the roads. Results on synthetic and real data show the interests of our method: the most salient curves such as the roads in satellite and aerial images or the vessels in 2D medical angiogram are exactly detected and the curves are continuous.

References

[1] R. Neviata, Locating structures in aerial images, *IEEE Trnas. PAMI*, pp. 476-484, Sept. 1982.

[2] F. Wang and R. Newkirk, A knowledge-based system for high-way network extraction, *IEEE Trans. Geosicence and Remote Sensing*, Vol. 26, Sept. 1988.

[3] I. Estival and H. Le Men, detection of linear networks on satellite images, *Proc. Conf. Pattern Recognition*, pp. 856-858, Oct. 1986.

[4] R.O. Duda and P.E. Hart, *Pattern Calssification and Scene Analysis*, New York: John Wiley Sons, 1973.

[5] M. Fischler, H. Tenenbaum, and H. Wolf, Detection of roads and linear structures in low-resolution aerial imagery using a multi-source knowledge integration technique, *Computer Graphics and Image Processing*, Vol. 15, pp. 201-223, 1981.

[6] Donald Geman and B. Jedynak, An active testing model for tracking roads in satellite images, *IEEE Trnas. PAMI*, Vol. 18, pp.1-14, 1996.

[7] Qifa Ke, Xiao Jing, Yang Zhiyong, Songde MA, Energy-based method for road extraction from satellite images, *Technic Report of National Lab of Pattern Recognition*,1996.

[8] J. M. Henderson and R.E. Quandt, *Microeconomic Theory*, A Mathematical Approach. 3rd, McGraw-Hill Book Co. 1985.

[9] Yang Zhiyong and Ma Songde, A phenomenological approach to salient maps and illusory contours, To appear in *Network: Computation in Neural Systems*.

[10] M.Kass, A.Witkin and D.Terzopoulos, Snakes: Active Contour Models, *Proceedings 1st Inter. Conf. on Computer Vision*, London, Englan, 1987.

[11] Song Chun Zhu, Region Competition: Unifying Snakes, Region Growing, and Bayes/MDL for Multi-band Image Segmentation, Technical Report no. 94-10, Harvard Robotics Laboratory.

[12] N.J. Hicks, Notes on Differential Geometry, D. Van Nostrand, Princeton, 1965.

[13] Daniel M. Wuescher and K.L. Boyer, Robust contour segmentation using a constant curvature criterion, *IEEE Trans. PAMI*, Vol. 13, pp. 41-51, 1991.

[14] M. Fischler and R.C. Bolles, Perceptual organization and curve partitioning, *IEEE Trans. PAMI-8*, pp. 100-105,1986.

[15] Paul L. Rosin and Geoff A. W. West, Nonparametric segmentation of curves into various representations, *IEEE Trans. PAMI*, Vol. 17, pp.1140-1153, 1995.

figure 1a

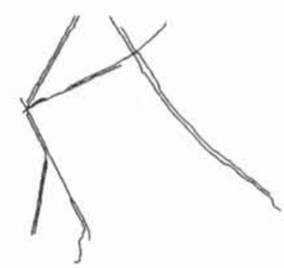

figure 1b

figure 2a

figure 2b

figure 3a

figure 3b